$$e_{aq}^- + N_2H_5^+ \longrightarrow H + N_2H_4 \qquad (14a)$$

$$e_{aq}^- + N_2H_5^+ \longrightarrow H_2 + \cdot N_2H_3 \qquad (14b)$$

$$H + N_2H_5^+ \longrightarrow H_2 + \cdot N_2H_4^+ \qquad (15)$$

The available results cannot distinguish between reactions 14a and 14b, and it should prove interesting to look for a competition for H atoms between reaction 15 and other added H-atom scavengers.

The marked dependence of the rate constant for reaction of e_{aq}^- with methyl-substituted hydrazine derivatives upon the state of protonation of the hydrazines and the dissociation constant are presented in Table I and Figure 1. Quantitatively, the electron affinity of these hydrazines does not correlate with the electron affinity of other inorganic protonic acids (*e.g.*, NH_4^+, $H_2PO_4^-$, $H_2PO_3^-$, NH_3OH^+). Presumably, in order to conform to the Brønsted relation the nature of the interaction (and therefore *primary* intermediates) between the hydrated electron and the inorganic acids must be similar.

Acknowledgment. A gift of trimethylhydrazine was received from Dr. K. Kustin of Brandeis University.

Electronic Spectra, Photochemistry, and Autoxidation Mechanism of the Sulfite–Bisulfite–Pyrosulfite Systems. The SO_2^-, SO_3^-, SO_4^-, and SO_5^- Radicals

E. Hayon,*[1a] A. Treinin,[1b,c] and J. Wilf[1c]

Contribution from the Pioneering Research Laboratory,
U. S. Army Natick Laboratories, Natick, Massachusetts 01760,
and the Department of Physical Chemistry, Hebrew University,
Jerusalem, Israel. *Received April 22, 1971*

Abstract: The electronic spectrum and the photochemistry of the sulfite–bisulfite–pyrosulfite systems in solution were investigated. The effects of pH, concentration, and environment upon the electronic spectrum were studied, and information was derived on some thermodynamic properties of the system and on the nature of the electronic transitions involved. Above 190 nm only HSO_3^- displays a charge-transfer-to-solvent (CTTS) band, but there is efficient ionization of the SO_3^{2-} ion on excitation within its intramolecular transition. The chain oxidation of sulfite ions in solution can lead to fast removal of oxygen from the system thus permitting the observation of the strong transient absorption of e_{aq}^- in such "air-containing" solutions. A mechanism for the autoxidation is proposed: $SO_3^{2-} + h\nu \rightarrow SO_3^- + e_{aq}^- (+ O_2 \rightarrow O_2^-)$; $SO_3^- + O_2 \rightarrow SO_5^-$; $SO_5^- + SO_3^{2-} \rightarrow SO_4^- + SO_4^{2-}$; $SO_4^- + SO_3^{2-} \rightarrow SO_4^{2-} + SO_3^-$, and termination reactions of the radicals. Some of the species may be present in their acidic forms. This mechanism is based on results concerning the radicals SO_3^-, SO_4^-, and SO_5^-. Information on these radicals was obtained from the flash photolysis of SO_3^{2-} and $S_2O_6^{2-}$, and from the pulse radiolysis of SO_3^{2-}, $S_2O_8^{2-}$, and HSO_5^-. No direct evidence is presented for the role of SO_4^- radicals in the chain reaction, but it is inferred from the nature of the inhibition induced by alcohols (SO_3^- and SO_5^- are relatively inert to alcohols) and from the production of O_3^- in alkaline solutions. The photolysis of $S_2O_5^{2-}$ leads to the formation of SO_2^- radicals. The flash photolysis of $S_2O_5^{2-}$ has provided new information on this radical. A survey is presented on some of the properties of the oxyanions and oxyradicals of sulfur. The absorption maxima, extinction coefficients, decay kinetics, and reactivity of the radicals SO_2^-, SO_3^-, SO_4^-, and SO_5^- are included.

The photolysis and oxidation (both thermal and photochemical) of sulfite ions have long been considered to involve electron transfer as a primary process.[2–4] This view was strongly supported by flash photolysis work,[5] which revealed the transient absorption of SO_3^- radicals in the uv region. In parallel, a strong short-lived absorption appeared around 700 nm, which closely resembles that of solvated electrons.[5] However, its appearance in "oxygen-containing" sulfite solutions in both pulse radiolysis and flash photolysis experiments has led to its assignment to an electron adduct.[5,6] It was later suggested by Devonshire and Weiss[7] that the light-induced chain oxidation of sulfite can lead to the fast removal of O_2 from the solution, and that the 700-nm band is indeed due to solvated electrons. This has been verified by our preliminary experiments, which also indicate that e_{aq}^- is rather inert

---

(1) (a) Natick Laboratories; (b) National Academy of Science–National Research Council Research Associate at Natick; (c) Hebrew University.

(2) (a) F. Haber, *Naturwissenschaften*, **19**, 450 (1931); (b) J. Franck and F. H. Sitzber, *Preuss. Akad. Wiss.*, 250 (1931); (c) F. Haber and O. H. Wansbrough-Jones, *Z. Phys. Chem., Abt. B*, **18**, 103 (1932).

(3) (a) H. L. J. Backstrom, *J. Amer. Chem. Soc.*, **49**, 1460 (1927); (b) H. N. Alyea and H. L. J. Backstrom, *ibid.*, **51**, 90 (1929); (c) H. L. J. Backstrom, *Z. Phys. Chem., Abt. B*, **25**, 122 (1934).

(4) (a) W. A. Waters, "The Chemistry of Free Radicals," 2nd ed, Clarendon Press, Oxford, 1948, p 234; (b) G. Pannetier and P. Souchay, "Chemical Kinetics," Elsevier, Amsterdam, 1967, p 240; (c) N. Semenoff, "Chemical Kinetics and Chain Reactions," Clarendon Press, Oxford, 1935, p 377; (d) for a very detailed survey of early research on autoxidation of sulfite, see "Gmelins Handbuch der anorganische Chemie," 8th ed, Teil No. B3, Verlag Chemie, Weinheim, 1963.

(5) L. Dogliotti and E. Hayon, *J. Phys. Chem.*, **72**, 1800 (1968).

(6) G. E. Adams, J. W. Boag, and D. B. Michael, *Proc. Chem. Soc., London* 411 (1964); *Trans. Faraday Soc.*, **61**, 1674 (1965).

(7) D. Devonshire and J. Weiss, *J. Phys. Chem.*, **72**, 3815 (1968).

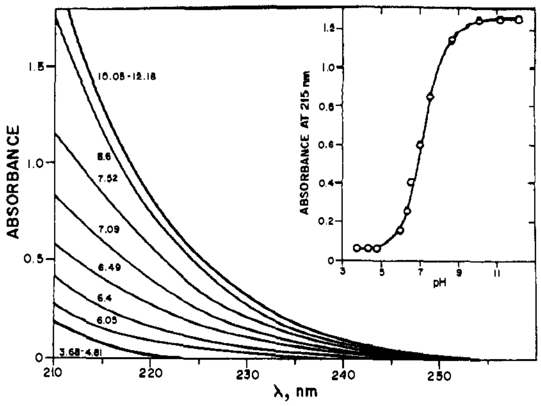

Figure 1. Absorption spectra of a 5×10^{-3} *M* aqueous bisulfite solution at various pH values, 20°, 1-mm optical path. Insert: absorbance at 215 nm as a function of pH.

to $SO_3{}^{2-}$ ions but reacts more rapidly with $HSO_3{}^-$, probably by a proton-transfer mechanism (see below).

The formation of solvated electrons from excited anions is often considered as evidence for the charge-transfer-to-solvent (CTTS) nature of the excited state. But this approach can be misleading, as is clearly indicated by the phenolate and naphtholate anions, which give rise to high yields of solvated electrons from internally excited states[8] (reactions which are analogous to preionization processes). For this reason we investigated the nature of the excited states of $SO_3{}^{2-}$ and $HSO_3{}^-$ by purely spectroscopic methods, through the study of environmental effects on their absorption spectra (section II.A). Our results also provide some thermodynamic data on the equilibria

$$HSO_3{}^- \rightleftharpoons H^+ + SO_3{}^{2-}$$

$$2HSO_3{}^- \rightleftharpoons S_2O_5{}^{2-} + H_2O$$

The $SO_3{}^-$ radical has been postulated as a chain carrier in all the mechanisms proposed for the autoxidation of sulfite.[2-4] A reaction involving $SO_3{}^-$ and O_2 appears to take place, and formation of $SO_5{}^-$ (or HSO_5) was suggested.[3c] However, no evidence has been presented for the participation of $SO_5{}^-$ or other proposed intermediates (OH,[2] $HSO_5{}^-$,[3c] HO_2[9]) in this reaction, which is one of the most famous chain reactions in solution. We have therefore conducted a detailed study on the $SO_3{}^-$ radical (produced by flash photolysis and pulse radiolysis of sulfite ions, and by flash photolysis of $S_2O_6{}^{2-}$) and obtained a better description of its spectrum and some basic information on its reactivity—in particular, its reaction with O_2 to produce a new intermediate. The identification of the latter as $SO_5{}^-$ (or HSO_5) is based on the results obtained by radiolysis of Caro's salt (section II.B.3).

Additional information on this chain reaction has been obtained from (a) the flash photolysis of alkaline sulfite solutions and (b) the inhibiting effect of alcohols. These results together with some new data on the properties of $SO_4{}^-$ (section II.B.5) lead us to postulate that the $SO_4{}^-$ radical also acts as a chain carrier in the oxidation of sulfite.

The bisulfite ion $HSO_3{}^-$ exists in equilibrium with $S_2O_5{}^{2-}$ which absorbs strongly at ~255 nm.[10] From this and the flash photolysis of $S_2O_4{}^{2-}$, some valuable information could be derived on the properties of the $SO_2{}^-$ radical (section II.B.4). Thus the present work provides knowledge on the oxysulfur radicals $SO_n{}^-$, where $n = 2–5$. The data obtained concerning these radicals and the parent oxyanions, from which they are generated, have been summarized.

I. Experimental Section

Materials. Na_2SO_3, $NaHSO_3$, $K_2S_2O_5$, and $K_2S_2O_8$ of research reagent grade were used without further purification. The effect of recrystallizing Na_2SO_3 from water-CH_3CN solution was tested: no change in the shape of the absorption spectrum was detected, but some reduction in intensity occurred which could be attributed to oxidation. To minimize oxidation, only fresh solutions were employed. Unless otherwise stated, before dissolving sulfite or pyrosulfite at pH <8 care was taken to remove O_2 from water (containing the proper buffer) by vigorous bubbling with prepurified N_2.

Tetraethylammonium sulfite was used as a source of $SO_3{}^{2-}$ and $HSO_3{}^-$ in organic solvents. It was prepared by dissolving SO_2 in a solution of $N(C_2H_5)_4OH$ which was kept at 0° to prevent oxidation. (SO_2 was generated by treating Na_2SO_3 with H_2SO_4 and rinsed by bubbling through a solution of $Ba(OH)_2$; $N(C_2H_5)_4OH$ was freed from some yellow impurities by several extractions with CH_3CN.) pH 9.5 was chosen as the end point for preparation of $[N(C_2H_5)_4]_2SO_3$. The solution was then evaporated under vacuum and the material crystallized by cooling to 0° and adding CH_3CN. The white hygroscopic crystals were rinsed several times with CH_3CN and dried under vacuum. The absorption spectrum of the product was almost identical with that of Na_2SO_3 under the same conditions.

Organic solvents were of spectroscopic grade. The drying of CH_3CN and conversion of $SO_3{}^{2-}$ into $HSO_3{}^-$ in organic solvents were performed as described elsewhere.[11] Water was purified by triple distillation, radiolysis, and photolysis, and D_2O (99.7%, Fluka, Puriss) was used without further purification.

For spectroscopic measurements phosphate and acetate buffers were used. For the flash and pulse experiments only borate buffers were employed.

$Na_2S_2O_4$ of technical grade (Baker and Adamson) was used without further purification, since solutions of low concentration were studied (~10^{-4} *M*), and the products of its decomposition (produced during the experimental run) had no effect on the flash photolysis results. The spectrum of this solution (N_2 saturated with 0.1 *M* NaOH at 4°) displayed an intense band, λ_{max} 317 nm and $\epsilon_{max} > 6 \times 10^3$ M^{-1} cm^{-1}. (Owing to thermal decomposition, no accurate value of ϵ_{max} could be determined.) These parameters are in agreement with previous results.[12]

Solutions of $KHSO_5$ and $NaHSO_5$ were prepared by the method of Mariano,[13] neutralizing the acid with KOH or NaOH, respectively. These solutions contained high concentrations of sulfates and unknown concentrations of $S_2O_8{}^{2-}$ and H_2O_2.

Measurements. Spectroscopic measurements, flash photolysis, and pulse radiolysis experiments were conducted as described in ref 11 and 14. For $Na_2S_2O_4$ solutions a special bubbler was used equipped with a cooling jacket filled with crushed ice. First the 0.1 *M* NaOH solution was chilled, O_2 was removed by bubbling with N_2, and a weighed quantity of $Na_2S_2O_4$ was then added. A sample of the solution was taken to measure its spectrum before connecting the bubbler to the photolytic cell.

For determination of p*K* ($HSO_3{}^-$), the pH was measured with a Metrohm pH meter (ΔpH ±0.01).

All the spectra recorded are the average of at least three runs with maximum scatter (in the case of some weak transients produced by flash) of ±20%. The quartz cells used had optical path lengths of 20 and 2 cm in the flash photolysis and pulse radiolysis experiments, respectively.

II. Results and Discussion

(A) The Electronic Spectra of $SO_3{}^{2-}$, $HSO_3{}^-$, and $S_2O_5{}^{2-}$. Figure 1 shows the absorption spectrum of

---

(8) (a) J. Jortner, M. Ottolenghi, and G. Stein, *J. Amer. Chem. Soc.*, **85**, 2712 (1963); M. Ottolenghi, *ibid.*, **85**, 3557 (1963); (b) C. R. Goldschmidt and G. Stein, *Chem. Phys. Lett.*, **6**, 299 (1970).

(9) J. Weiss, *Annu. Rep. Progr. Chem.*, **44**, 60 (1947).

(10) R. M. Golding, *J. Chem. Soc.*, 3711 (1960).

(11) A. Treinin and J. Wilf, *J. Phys. Chem.*, **74**, 4131 (1970).

(12) E. M. Kosower and S. W. Bauer, *J. Amer. Chem. Soc.*, **82**, 2191 (1960).

(13) M. H. B. Mariano, *Advan. Chem. Ser.*, **No. 81**, 182 (1968).

(14) (a) M. Langmuir and E. Hayon, *J. Phys. Chem.*, **71**, 3808 (1967); see also (b) L. Dogliotti and E. Hayon, *ibid.*, **71**, 2511 (1967); (c) M. Simic, P. Neta, and E. Hayon, *ibid.*, **73**, 3794 (1969); E. Hayon, *J. Chem. Phys.*, **51**, 4881 (1969).

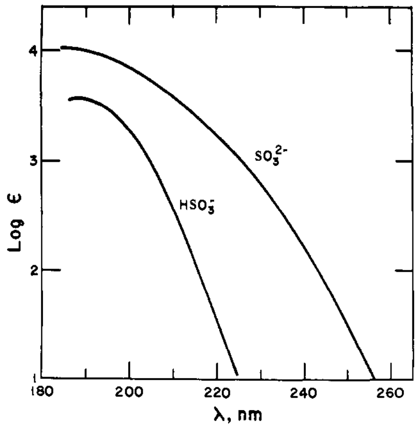

Figure 2. Electronic spectra of HSO_3^- and SO_3^{2-} ions in water.

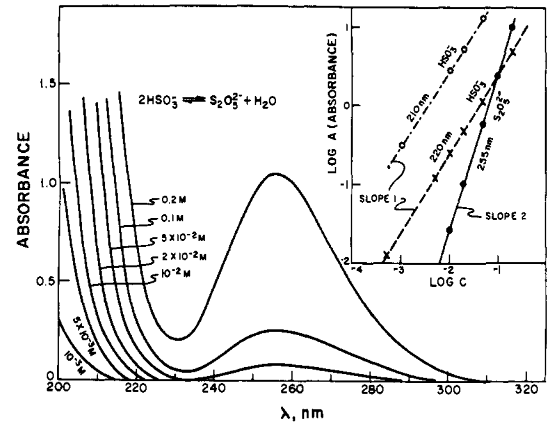

Figure 3. Absorption spectra of different concentrations (10^{-3}–0.2 M) of bisulfite ions at pH 3.9, 20°, 1-mm optical path. Insert: log (absorbance) *vs.* log [HSO_3^-] at 210, 220, and 255 nm.

5 × 10^{-3} M sulfite in water at various pH values, and a typical "titration curve" (insert). From such curves at different temperatures, the equilibrium constant, $K_d = A_H + A_{SO_3^{2-}}/A_{HSO_3^-}$, and related thermodynamic data could be determined. The method of computation is described in ref 11. The results are summarized in Table I, together with some previous data for comparison.

Table I. Thermodynamic Data for the Equilibrium $HSO_3^- \rightleftharpoons H^+ + SO_3^{2-}$

	Temp, °C	Present work	Previous data[a]
pK	5	7.05 ± 0.02	
	15	7.15 ± 0.02	
	25	7.20 ± 0.02	7.15, 7.205, 7.20
	35	7.30 ± 0.03	
	50	7.35 ± 0.03	
ΔG,° kcal/mol	25	9.8 ± 0.6	9.8
ΔH°, kcal/mol	25	−2.7 ± 0.3	≤−2.3
ΔS°, eu	25	−42 ± 3	

[a] The data were taken from *Chem. Soc., Spec. Publ.*, No. **17**, Table 55 (1964). This refers to zero ionic strength. For more data, consult this table.

Figure 2 records the spectra of SO_3^{2-} and HSO_3^- at 20°. No maxima or "shoulders" could be discerned above 200 nm; HSO_3^- reaches its peak at ~190 nm and SO_3^{2-} at a somewhat shorter wavelength. Some previously reported peaks of SO_3^{2-}[10,15,16] and HSO_3^-[10] are probably due to impurities or stray light effects. False peaks close to 200 nm which shift to longer wavelengths with rise in concentration (as claimed for HSO_3^- [10]) are typical stray-light effects.[17]

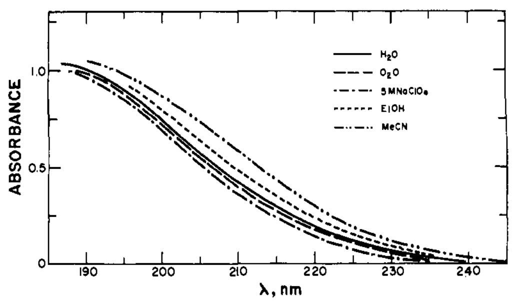

Figure 4. Absorption spectra of 10^{-3} M tetraethylammonium sulfite in various solvents, 20°, 1-mm optical path.

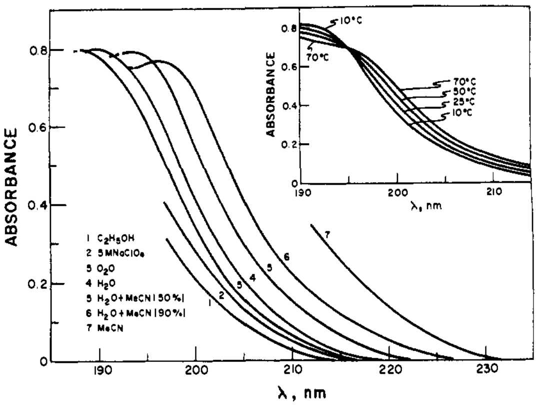

Figure 5. Absorption spectra of 2 × 10^{-3} M HSO_3^- ions in solvents of various composition, 20°, 1-mm optical path. Insert: effect of temperature on the absorption of 2 × 10^{-3} M HSO_3^- in H_2O.

SO_3^{2-} in water was found to obey Beer's law in the range 5 × 10^{-5}–0.5 M over the whole wavelength region studied. The behavior of HSO_3^- is more complicated (see Figure 3): at $\lambda \lesssim 220$ nm, Beer's law is valid over a considerable range of concentration, but at longer wavelengths HSO_3^- displays the characteristic buildup of $S_2O_5^{2-}$ as its concentration rises,[10,15] with absorbance (measured at λ_{max} 255 nm) being proportional to $[HSO_3^-]^2$. This behavior is illustrated by logarithmic correlations in the insert of Figure 3. From the intercept of the 255-nm line, $K_1\epsilon_{255} = 270$ M^{-1} was determined, where K_1 is the equilibrium constant of

$$2HSO_3^- \rightleftharpoons S_2O_5^{2-} + H_2O \qquad (1)$$

This value is in good agreement with previous data.[10] The validity of Beer's law in the region ~200–220 nm implies that (a) $S_2O_5^{2-}$ does not absorb appreciably in this region; (b) K_1 is small so that at 0.2 M (the highest concentration studied) only little HSO_3^- is converted to $S_2O_5^{2-}$ ($K_1 \sim 7 \times 10^{-2}$ M^{-1} was determined by Golding[10]); and (c) contrary to a previous report,[10] the uv

---

(15) Early works on this subject are summarized in "Gmelins Handbuch der anorganische Chemie," 8th ed, Vol. 9, Teil No. B2, Verlag Chemie, Weinheim, 1960, p 413.

(16) S. P. Tandon and K. Tandon, *Indian J. Pure Appl. Phys.*, 8, 199 (1970).

(17) G. H. Beaven, E. A. Johnson, H. A. Willis, and R. G. Miller, "Molecular Spectroscopy," Heywood, London, 1961, p 65.

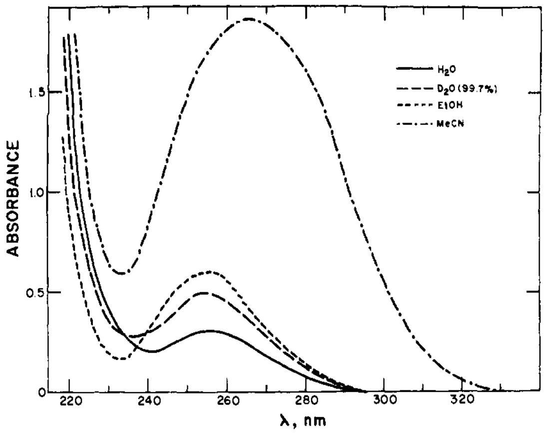

Figure 6. Absorption spectra of 3.5 × 10^{-2} M tetraethylammonium bisulfite in different solvents, 10°, 1-cm optical path.

spectrum does not reflect isomerization of HSO$_3^-$ up to 0.2 M.

Figures 4, 5, and 6 show solvent effects on the spectra of SO$_3^{2-}$, HSO$_3^-$, and S$_2$O$_5^{2-}$, respectively. The validity of Beer's law was verified with NEt$_4$HSO$_3$ and (NEt$_4$)$_2$SO$_3$ in CH$_3$CN and ethanol in the range 10^{-4}M–10^{-2} M. Only HSO$_3^-$ displays the characteristic behavior of a CTTS band; this is clearly demonstrated in Figure 7, where the transition energies at specified extinction coefficients are plotted against the CTTS value[18] of the solvent. The temperature effect (Figure 5, insert) is also in agreement with this assignment.[19] (There is indication for a second overlapping band at elevated temperatures; see Figure 5.) The difference $h\nu_{\max} - h\nu_{\epsilon 1}$ of HSO$_3^-$ in water is ~25 kcal, close to that of other CTTS bands.[20] On the other hand, the absorption band of SO$_3^{2-}$ is considerably wider (Figure 2) and undergoes a regular blue shift with increase of polarity (Figure 4). Thus SO$_3^{2-}$ resembles the halate ions,[21] which have isoelectronic valence shells. By analogy, the assignment of this band to $^1A_1 \leftarrow {}^1A_1$ transitions[16] seems plausible.

The spectrum of S$_2$O$_5^{2-}$ has low solvent sensitivity; but there is a pronounced intensification with decrease of polarity (Figure 6), which most likely reflects an increase in the equilibrium constant K_1. Decrease of temperature also brings about the same effect. Assuming that ϵ_{255} does not change with temperature, the enthalpy change in reaction 1 could be calculated by plotting log ($K_1\epsilon_{255}$) against $1/T$: $\Delta H_1 \sim -0.8$ kcal.

The vertical ionization potential E of HSO$_3^-$ could be calculated from the transition energy of its CTTS band ($h\nu_{\max}$ = 150 kcal/mol) and its thermochemical radius ($R_{\mathrm{HSO_3^-}} \sim 1.8$ Å; it was assumed to be smaller by 0.2 Å than that of SO$_3^{2-}$).[11] The value obtained is $E_{\mathrm{HSO_3^-}} \sim 3.5$ eV. Thus in its electron-transfer properties HSO$_3^-$ is close to Br$^-$.

The question arises as to the location of the CTTS band of SO$_3^{2-}$. Usually the first CTTS band of XO$_n^{2-}$ has $h\nu_{\max}$ lower than that of HXO$_n^-$.[19] A possible answer is that it is located at longer wavelengths, and the broad absorption displayed by SO$_3^{2-}$ is due to the overlap of two bands. If this is the case, then the contribution of the CTTS band to the total absorption must be relatively small, since there is no indication of any specific solvent effects, even though these effects are usually much more pronounced than those of internal transitions.

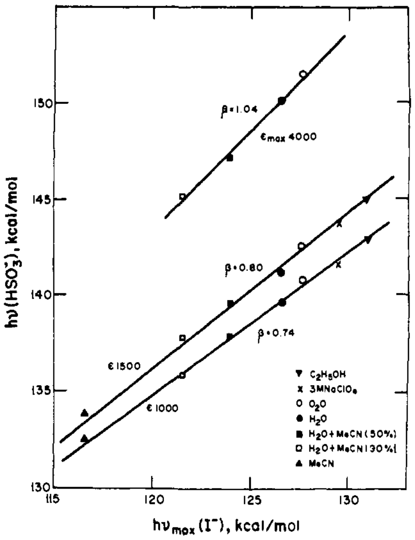

Figure 7. Plot of $h\nu$(HSO$_3^-$) *vs.* $h\nu_{\max}$(I$^-$) in various solvents.

(B) Intermediates. (1) Solvated Electrons. The assignment of the 700-nm transient species produced in the flash photolysis and pulse radiolysis of SO$_3^{2-}$ ions to the solvated electrons has been established by investigating its spectral and chemical properties. The parameters of this band are $\lambda_{\max}$ 700 ± 20 nm, $\epsilon_{\max}$ 1.8 × 10^4 M^{-1} cm^{-1}. The latter was obtained from pulse radiolysis experiments by simple dosimetry (see Experimental Section) and from flash photolysis experiments by measuring the absorbance ratio $A^{700}/A^{280}_{\mathrm{SO_3^-}}$ (extrapolated to zero time), assuming equal amounts of both transients and using the value $\epsilon^{280}_{\mathrm{SO_3^-}}$ = 630 M^{-1} cm^{-1} (section II.B.2). These parameters closely resemble that of e$_{\mathrm{aq}}^-$. The same applies to the chemical reactivity of this transient. Its reactions with NO$_3^-$ and N$_2$O were studied in pulsed and flashed solutions, respectively. The rate constants determined were $k_{\mathrm{NO_3^-}}$ = 1.1 ± 0.15 × 10^{10} M^{-1} sec^{-1} (corrected for ionic strength effect) and $k_{\mathrm{N_2O}} \sim 2 \times 10^9$ M^{-1} sec^{-1}. (The latter is an approximate value, because in this case the oscilloscope traces were not corrected for scattered flash light.) Comparison of these values with available data for e$_{\mathrm{aq}}^-$ [22] shows the resemblance in chemical reactivity.

As already described,[5,6] the 700-nm band was readily observed in air-saturated solutions of 10^{-2} M Na$_2$SO$_3$. However, on lowering the concentration of SO$_3^{2-}$ below ~10^{-3} M in the flash experiments or ~2 × 10^{-4} M in the pulse experiments, this transient could no longer be detected. The same effect was observed at somewhat higher concentrations of SO$_3^{2-}$ by using solutions saturated with O$_2$. Simultaneous with the suppression of e$_{\mathrm{aq}}^-$, the absorption in the uv region showed considerable enhancement, mainly due to the generation of O$_2^-$ (section II.B.3).

A simple analysis has shown that no oxygen is left after the flash in solutions where solvated electrons

---

(18) I. Burak and A. Treinin, *Trans. Faraday Soc.*, **59**, 1490 (1963).

(19) M. J. Blandamer and M. F. Fox, *Chem. Rev.*, 70, 59 (1970).

(20) H. L. Friedman, *J. Chem. Phys.*, 21, 319 (1953).

(21) A. Treinin and M. Yaacobi, *J. Phys. Chem.*, **68**, 2487 (1964).

(22) M. Anbar and P. Neta, *Int. J. Appl. Radiat. Isotop.*, **18**, 493 (1967).

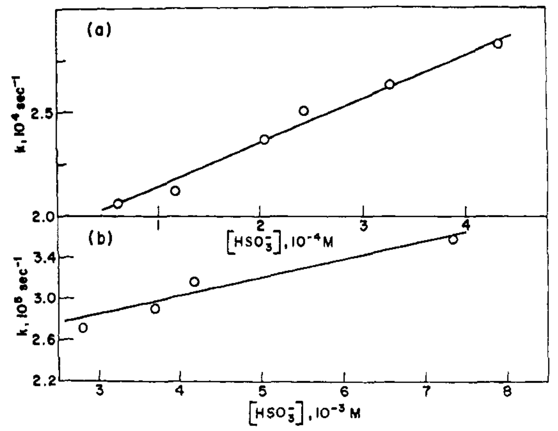

Figure 8. Pseudo-first-order decay rate of e_{aq}^- as a function of $[HSO_3^-]$ determined from flash photolysis (a) and pulse radiolysis (b) experiments.

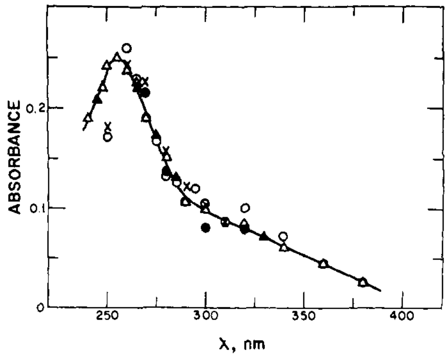

Figure 9. Absorption spectrum of the SO_3^- radical in aqueous solution obtained by pulse radiolysis [2 m*M* sulfite, N_2O, pH 10.3 (Δ) and 5.41 (▲)] and flash photolysis of (○) 0.3 m*M* sulfite, N_2O, pH 9.8, read 200 μsec after flash, multiplied by 5 for normalization; (●) 3.8 m*M* sulfite, N_2, pH 6.3, read 100 μsec after flash multiplied by 16; (×) 0.1 *M* $S_2O_6^{2-}$, N_2, pH 8.8, read 200 μsec after flash, multiplied by 24.

could be detected. By measuring the change in optical absorbance of sulfite after one flash, it was found that the light-induced depletion of SO_3^{2-} was about twice the initial concentration of O_2. For example, starting with 1.06×10^{-3} *M* and 2.2×10^{-3} *M* Na_2SO_3 solutions, each saturated with air (2.5×10^{-4} *M* O_2), their concentrations were reduced by flashing to 6.2×10^{-4} *M* and 1.75×10^{-3} *M*, respectively; with 6×10^{-3} *M* Na_2SO_3 saturated with O_2 (1.3×10^{-3} *M*), the depletion was 2.7×10^{-3} *M*. Since the stoichiometry of the oxidation is[3]

$$2SO_3^- + O_2 \longrightarrow 2SO_4^{2-} \tag{2}$$

the results indicate that in effect all the oxygen was removed from these solutions by one flash. In fact, the relatively high yield of solvated electrons observed after flash (about 1 μ*M*) implies that in these cases the chain reaction was essentially completed at the beginning of the flash. Assuming a chain length of 10^4, about 5×10^{-8} einstein/l. is necessary to consume all the oxygen in air-saturated solutions, which is only ~5% of the light absorbed.

In agreement with this interpretation, a striking indirect effect of the addition of alcohols on e_{aq}^- was detected. In air-saturated solutions, under conditions where the 700-nm band was readily detected after the flash, it could be completely suppressed by low concentrations of alcohols. Thus no electrons could be detected in air-containing solutions of 10^{-2} *M* Na_2SO_3 and 2×10^{-4} *M* isopropyl alcohol at pH 9.7. The same effect was also obtained with ethanol and methanol, but at higher concentrations. The reason for this effect is simple: by inhibiting the chain reaction,[3] the alcohols can prevent the full consumption of oxygen in the solution. (For further discussion of the inhibiting effect, see section II.C.)

Close to its threshold of detection (*e.g.*, with air-saturated 10^{-3} *M* Na_2SO_3) the 700-nm band appeared to be very sensitive to impurities. By somewhat shortening the chain length, impurities can prevent total removal of O_2. However, in those cases where e_{aq}^- could not be detected after the first flash, a second flash was usually sufficient to produce the strong 700-nm band.

In all the flash photolysis experiments, the decay of e_{aq}^- was first order, although no reaction of e_{aq}^- with SO_3^{2-} could be detected: the rate of decay hardly changed on raising $[SO_3^{2-}]$ from 10^{-4} to 10^{-2} *M*. Thus the first-order decay of e_{aq}^- at pH >9 reflects its reaction with some impurities. In the pulse radiolysis experiments, where the reaction $e_{aq}^- + e_{aq}^-$ can effectively compete with impurities, e_{aq}^- was found to decay with kinetics which appeared to be a mixture of first and second orders.

On lowering the pH, the reaction of e_{aq}^- with HSO_3^- (10^{-3}–10^{-1} *M*) could be followed in the pH range 8.0–8.5, using both pulse and flash techniques (with proper corrections for scattered light from the flash). The rate constant of the pseudo-first-order decay of e_{aq}^- was found to vary linearly with HSO_3^- concentration (Figure 8). The latter was calculated using $pK_1 = 7.2$, and the rate constants were corrected for ionic strength effect.[23a] (The pulse radiolysis data refer to decays which are at least three times faster than the decay at pH >9.) From the slopes of the lines (Figure 8), the rate constant of

$$e_{aq}^- + HSO_3^- \longrightarrow \text{products} \tag{3}$$

was determined as $k_3 = (2 \pm 1) \times 10^7\ M^{-1}\ \text{sec}^{-1}$.

Reaction 3 can occur in two possible ways

$$e_{aq}^- + HOSO_2^- \longrightarrow H + SO_3^{2-} \tag{4}$$

$$e_{aq}^- + HOSO_2^- \longrightarrow OH^- + SO_2^- \tag{5}$$

We believe that e_{aq}^- decays by reaction 4 for the following reasons. (a) SO_2^- rapidly dimerizes to $S_2O_4^{2-}$ (section II.B.4), but the latter could not be detected in this series of experiments.[23d] (b) The rate constant for conversion of e_{aq}^- to H is expected to follow the Brønsted relation[23]

$$\log (k/p) \sim 10 - 0.5[pK - \log (q/p)] \tag{6}$$

For HSO_3^-, $p = 1$, $q = 3$, and $pK = 7.2$; therefore, the conversion should proceed with $k \sim 3 \times 10^6\ M^{-1}\ \text{sec}^{-1}$. This differs considerably from the experimental value, but the discrepancy is still within the scatter of some other data for this correlation. (According to

---

[23] (a) J. Rabani, *Advan. Chem. Ser.*, No. 50, 242 (1965); (b) J. Jortner, M. Ottolenghi, J. Rabani, and G. Stein, *J. Chem. Phys.*, 37, 2488 (1962); (c) G. Stein, *Isr. J. Chem.*, *Proc. Farkas Symp.*, in press. (d) The formation of $S_2O_4^{2-}$ could be detected after flashing 5 m*M* HSO_3^- at pH 3.7. Under these conditions, the reaction $H + HOSO_2^- \rightarrow H_2O + SO_2^-$ may occur. At lower $[HSO_3^-]$, H atoms probably react[2c] with SO_3^-.

Table II. Second-Order Rate Constants for the Decay of SO_3^- Radicals

Method	Conditions	λ, nm	$2k/\epsilon$	$2k$, M^{-1} sec^{-1}	$2k$ (I = 0), M^{-1} sec^{-1}
Flash photolysis of	2.5×10^{-4} *M*				
SO_3^{2-}–HSO_3^-	pH 9.5, N_2O satd	265	1.4×10^6	1.3×10^9	
	2.8×10^{-4} *M*				
	pH 9.8, N_2O satd	320	3.6×10^6	1.2×10^9	Av $(1.1 \pm 0.2) \times 10^9$
	3.0×10^{-4} *M*	270	1.4×10^6	1.1×10^9	
	pH 9.8, N_2O satd	255	1.2×10^6	1.2×10^9	
	3.5×10^{-3} *M*	260	1.3×10^6	1.3×10^9	
	pH 5.1, N_2 satd				
	4.9×10^{-3} *M*	260	8.3×10^5	8.3×10^8	
	pH 4.6, N_2 satd	270	1.1×10^6	8.7×10^8	
	4.9×10^{-3} *M*	260	1.2×10^6	1.2×10^9	
	pH 3.7, N_2 satd				
	10^{-2} *M*, pH 9.3	275	$(2.0 \pm 1.0) \times 10^6$	$(1.8 \pm 0.9) \times 10^9$	$(1.3 \pm 0.7) \times 10^9$
	N_2 or N_2O satd[a]				
Pulse radiolysis of	2×10^{-3} *M*				
SO_3^{2-}–HSO_3^-	pH 10.2, N_2O satd	255	9.8×10^5	1.0×10^9	
	2×10^{-3} *M*				8.5×10^8
	pH 5.4, N_2O satd	255	9.9×10^5	1.0×10^9	
Flash photolysis	0.1 *M*, pH 8.4	270	$(2.2 \pm 1.0) \times 10^6$	$(2.2 \pm 1.0)\ 10^9$	
of $S_2O_6^{2-}$	N_2 satd[b]	280	4.5×10^6	2.8×10^9	Av $(1.1 \pm 0.5) \times 10^9$
	0.1 *M*, pH 8.4				
	N_2 satd[c]	275	$(3.5 \pm 2) \times 10^6$	$(2.5 \pm 1.5) \times 10^9$	$(1.1 \pm 0.8) \times 10^9$
	0.1 *M* + 0.4 *M*	270	1.8×10^6	1.4×10^9	6×10^8
	ethanol, pH 8.8				
	N_2 satd				

[a] From ref 5. [b] Average of three runs. [c] From ref 24.

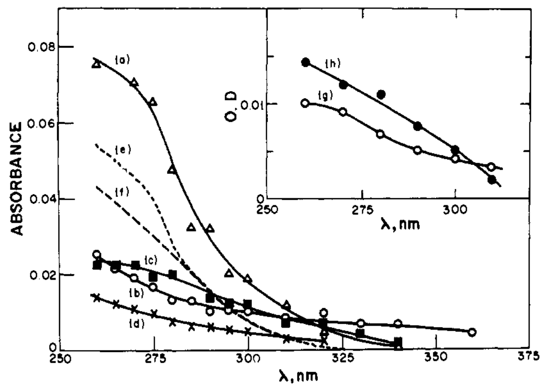

Figure 10. Transient spectra produced on flash photolysis of 0.3 m*M* Na_2SO_3 at pH 9.8 (absorbance read at 200 μsec after flash) in (a) air, 2.5×10^{-4} *M* O_2; (b) 2×10^{-2} *M* N_2O; (c) 8×10^{-5} *M* O_2 + 7×10^{-3} *M* N_2O; (d) spectrum of permanent product in air-saturated solution; (e) difference between curves a and c; (f) spectrum of O_2^- (from ref 25). Curves b and c were drawn to half scale. Insert: transient spectra produced on flash photolysis of 0.1 *M* $Na_2S_2O_6$, pH 8.8 in N_2 (g) and air (h); read 200 μsec after flash.

Stein,[23c] the discrepancy is due to a parallel process, where e_{aq}^- directly attacks the sulfur atom.)

These results imply that e_{aq}^- is efficiently produced from internally excited SO_3^{2-}, since no evidence for a CTTS band could be observed. The mechanism of this pre-ionization process is not clear. By using a 20% acetic acid filter it was found that wavelengths above 237 nm were also effective in producing solvated electrons in 10^{-2} *M* SO_3^{2-} at pH 9.8. Possible mechanisms are (a) CTTS excitation, probably by intersystem crossing, if we assume that a CTTS band is concealed in this wavelength region, and (b) fast protonation of the excited state and conversion to the CTTS state of HSO_3^-.

(2) SO_3^- Radical. Figure 9 shows the transient absorption spectrum produced from (a) the pulse radiolysis and flash photolysis of sulfite solutions, saturated with N_2O or N_2, at different pH values in the range 5.4–10.3, and (b) the flash photolysis of N_2-saturated solutions of $S_2O_6^{2-}$. These systems have already been studied in previous works,[5,6,24] but the reported spectrum appears to suffer from stray-light effects: the peak is not around 270 nm[5,24] but at 255 nm (Figure 9). (This effect can still be seen below 260 nm in these flash experiments, where the monitoring light is weaker than in the pulse experiments.)

Table II summarizes the kinetic data for the second-order decay of this transient absorption. The following conclusions can be drawn: (a) the absorption spectrum shown in Figure 9 belongs to one species, since the transient at 255 and 320 nm decays at the same rate; (b) the decay is hardly affected by pH in the range 4–10 (the spectrum also remains unchanged in this range; Figure 9); (c) the decay rate constant depends on sulfite concentration (column 5) (a constant value $2k = (1.1 \pm 0.2) \times 10^9$ M^{-1} sec^{-1} was found to apply to solutions with ionic strength ranging from 7×10^{-4} to 0.3, by assuming that the transient is a mononegative ion and correcting for ionic strength effect); and (d) the reaction between the transient and ethanol is relatively slow, $k \lesssim 2 \times 10^3$ M^{-1} sec^{-1}. A similar observation and rate was found with isopropyl alcohol (up to 0.5 *M*).

The mechanism leading to the formation of this transient, the effect of N_2O to double its yield[5] (this was also verified in the present work), and the above observations lend strong support to the assignment of this transient to the SO_3^- radical. Its spectral and kinetic parameters are summarized in the last section.

(3) SO_5^- Radical. Oxygen (when not totally consumed by the chain reaction) exerts a pronounced effect on the transient absorption produced in the flash photolysis of SO_3^{2-}. Below 300 nm, the absorption becomes appreciably stronger than in oxygen-free solutions, and the characteristic long-tailed spectrum of SO_3^- disappears (Figure 10, curves a and b; curve b was

---

(24) L. Dogliotti and E. Hayon, *Nature (London)*, **218**, 949 (1968).

derived from experiments with N_2O-saturated solutions and the absorption was drawn to half scale). The enhanced absorption is due largely to formation of O_2^-. This could be demonstrated in the photolysis of a $^1/_{100}$ O_2–N_2O mixture, so that e_{aq}^- was effectively scavenged by N_2O. The results are shown in Figure 10c. Here too the absorption was drawn to half scale because SO_3^-, the yield of which is doubled by N_2O (eq 7 and 9), appears to be the precursor of the new intermediate. In this way, curves a, b, and c correspond to equivalent amounts of sulfur radicals. The results indicate that SO_3^- reacts with O_2, and curve c represents the transient absorption from this reaction. Its second-order decay is slower than that of SO_3^-, with $2k = [(5 \pm 1) \times 10^5]\epsilon_{280}\ M^{-1}\ \mathrm{sec}^{-1}$. This was checked at pH 9–10 and $[SO_3^{2-}] = 1.\times 10^{-4}$–$4 \times 10^{-4}\ M$. The initial sequence of reactions in solutions containing oxygen appears to be

$$SO_3^{2-} \xrightarrow{h\nu} SO_3^- + e_{aq}^- \qquad (7)$$

$$e_{aq}^- + O_2 \longrightarrow O_2^- \qquad (8)$$

in the presence of N_2O

$$\begin{aligned} e_{aq}^- + N_2O &\longrightarrow N_2 + OH^- + OH \\ OH + SO_3^{2-} &\longrightarrow OH^- + SO_3^- \end{aligned} \qquad (9)$$

$$SO_3^- + O_2 \longrightarrow X \qquad (10)$$

The effect of O_2 on SO_3^- and the occurrence of a chain reaction could easily be demonstrated by exposing the same solution to a second or third flash: the characteristic transient absorption of SO_3^- emerged, with its faster decay rate. This was found to be the case in the presence or absence of N_2O, which shows that O_2^- does not play the role of a chain carrier. The same conclusion was reached by measuring the depletion of sulfite.

Curve a of Figure 10 is thus interpreted as the spectrum of $O_2^- + X$ produced in equimolar amounts. The decay rate of this absorption ($\tau_{1/2}$ ~2 msec at pH 9.8) is considerably faster than that of O_2^-,[25] with order between 1 and 2, which suggests that O_2^- also reacts with X. (For similar enhancement in the decay rate of O_2^-, see ref 26.) However, the difference between spectra a and c (curve e), although coinciding with the spectrum of O_2^- (curve f) up to ~280 nm, is considerably different at shorter wavelengths. (Curve f represents the spectrum of O_2^-, taken from ref 25, in amount equal to that of SO_3^-.)

The following results lead us to believe that the discrepancy is due to some error in determining the spectrum of X. The effect of O_2 on SO_3^- could also be established by studying the $S_2O_6^{2-}$ system. Figure 10 (insert) shows the transient absorption in absence and presence of O_2. These spectra are rather weak but the same general pattern was observed in four different runs. This system is chemically less complicated, since no chain reaction is involved. The relevant reaction in this case is

$$S_2O_6^{2-} \xrightarrow{h\nu} 2SO_3^- \qquad (11)$$

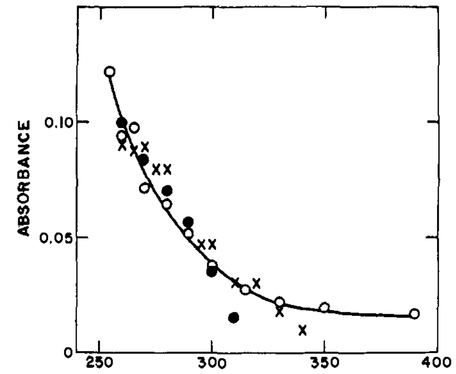

Figure 11. Absorption spectrum of SO_5^- radicals produced from (○) pulse radiolysis of 2 mM $KHSO_5$, pH ~6, N_2O; (×) flash photolysis of 0.3 mM Na_2SO_3, pH 9.8, $8 \times 10^{-5}\ M\ O_2 + 7 \times 10^{-3}\ M\ N_2O$, multiplied by 2 for normalization; and (●) air-saturated 0.1 M $Na_2S_2O_6$, multiplied by 7. Absorbance read 200 μsec after flash.

followed by reaction 10. Up to ~280 nm, the spectrum attributed to X (curve h) is similar to that displayed by the sulfite system, but it does not level off at shorter wavelengths. Moreover, the difference between curves a and h (properly normalized) resembles more closely the spectrum of O_2^-. The data concerning the decay kinetics of transient h are not conclusive, owing to the weakness of the absorption and the formation of a permanent product (see the end of this section). Second-order plots gave $2k = [(1.0 \pm 0.3) \times 10^6]\epsilon_{280}\ M^{-1}\ \mathrm{cm}^{-1}$, which is not far from the previous value. Therefore, curve h is considered to give a better representation of the spectrum of transient X. The reason for its distortion in the sulfite system is not clear.[27]

The simplest formula for the intermediate X is SO_5^- (or HSO_5)

$$SO_3^- + O_2 \longrightarrow SO_5^- \qquad (12)$$

Pulse radiolysis of Caro's salt was recently investigated and the spectrum of an intermediate with this formula was reported.[28a] It was produced by the reaction

$$OH + HSO_5^- \longrightarrow OH + HSO_5\ (\text{or } SO_5^-) \qquad (13)$$

with $k_{13} = 2.9 \times 10^8\ M^{-1}\ \mathrm{sec}^{-1}$. Its spectrum resembles that of X but it is somewhat flatter: both have nearly the same absorptivity at 310 nm (ϵ ~200 $M^{-1}\ \mathrm{cm}^{-1}$), but at 270 nm the spectrum reported by Roebke, *et al.*,[28a] has ϵ ~300 $M^{-1}\ \mathrm{cm}^{-1}$, compared with ~1000 $M^{-1}\ \mathrm{cm}^{-1}$ exhibited by X. For this reason, we repeated the pulse experiment. In general, our findings (Figure 11) are in agreement with previous results[28a] (including the formation of SO_4^- from the reaction of e_{aq}^- with HSO_5^-), but the spectrum of "SO_5^-" appears to be steeper. Figure 11 also includes the normalized spectrum of X; the agreement with the spectrum of X, as obtained from the flash photolysis of $S_2O_6^{2-}$, is satisfactory. Since impure solutions of Caro's salt were used (see Experimentsl Section), we could only determine a lower limit for the extinction coefficient, $\epsilon^{265}_{SO_5^-}$

---

(25) D. Behar, G. Czapski, J. Rabani, L. Dorfman, and H. Schwarz, *J. Phys. Chem.*, **74**, 3209 (1970).

(26) (a) J. R. Huber and E. Hayon, *ibid.*, **72**, 3820 (1968); (b) D. Behar, G. Czapski, and I. Duchovny, *ibid.*, **74**, 2206 (1970).

(27) The autoxidation of sulfite is a thermoluminescent process; see J. Stauff, H. Schmidkunz, and G. Hartman, *Nature* (*London*), **198**, 281 (1963). Light emission can lead to a decrease in transient absorption. This possibility should be examined.

(28) (a) W. Roebke, M. Renz, and A. Henglein, *Int. J. Radiat. Phys. Chem.*, **1**, 29 (1969); (b) K. Stockhausen, A. Fojtik, and A. Henglein, *Ber. Bunseges. Phys. Chem.*, **74**, 34 (1970).

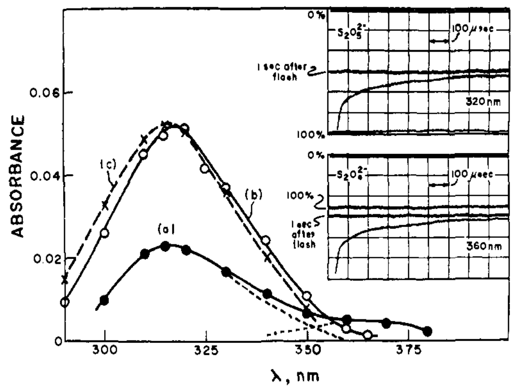

Figure 12. Spectral changes induced by flash photolysis of $S_2O_5^{2-}$ ions. A 60 m*M* bisulfite solution was used, pH 4.0, N_2 (1 atm), temperature = 20°, 240-nm cutoff filter (20% acetic acid): curve a read at 80 μsec and curve b at ~1 sec after flash; curve c is the normalized absorption spectrum of $Na_2S_2O_4$ in water, pH 13, temperature 4°. Oscilloscope traces: (top) $S_2O_5^-$ in 9.3 × 10^{-2} *M* HSO_3^-, N_2, 320 nm; (bottom) ~3.0 × 10^{-4} *M* $Na_2S_2O_4$ in 0.1 *N* NaOH, N_2, ~4°, 360 nm.

~560 M^{-1} cm^{-1}. There are no previous data on the decay kinetics of SO_5^-. In our experiments, the weak oscilloscope traces showed no simple order of decay, with $\tau_{1/2} \sim 3$ μsec with N_2O-saturated solutions, 2–10 m*M* HSO_5^-, 1 *M* Na_2SO_4. It is necessary to repeat these experiments with pure solutions (or to test the effect of various possible impurities, *e.g.*, H_2O_2) to establish the decay kinetics.

Addition of 0.2 *M* ethanol to air-containing solutions of $S_2O_8^{2-}$ at pH 9.1 had little effect on the intensity and the decay rate of the transient produced by flash photolysis (measured in the region 260–280 nm). At this pH, the peroxy radical of ethanol lives much longer and has a considerably higher absorption than SO_5^-.[28b] Thus the reaction SO_5^- + ethanol is relatively slow ($k \lesssim 10^3\ M^{-1}\ sec^{-1}$).

In all cases reported here where SO_5^- was presumably formed, weak, ill-defined, long-lived absorptions were observed in the 250–300-nm region. This is shown for the $SO_3^{2-} + O_2$ system in Figure 10, curve d. These absorptions are probably due to the products of reactions like $O_2^- + SO_5^-$ or $SO_5^- + SO_5^-$.

A marked "shoulder" displayed by the absorption spectrum of γ-irradiated solid persulfates has recently been assigned to SO_5^-.[29] Our results are not in accord with this assignment.

Some preliminary work was conducted on the flash photolysis of $KHSO_5$. A high yield of SO_4^- was observed, probably resulting from the reaction

$$HSO_5^- \xrightarrow{h\nu} SO_4^- + OH \qquad (14)$$

However, SO_5^- (which should subsequently be generated by reaction 13) could not be detected. The reason is not clear.

(4) SO_2^- Radical. Flash photolysis of HSO_3^- at relatively low concentration ($\lesssim 5 \times 10^{-3}$ *M*) gives rise to the same uv transient absorption as produced from SO_3^{2-}. But on raising its concentration, when the buildup of $S_2O_5^{2-}$ becomes apparent due to $2HSO_3^- \rightleftharpoons S_2O_5^{2-} + H_2O$, new features emerge. Figure 12 shows the results obtained with 6 × 10^{-2} *M* bisulfite at pH ~4, using a 20% acetic acid filter to cut off light below 240 nm. Under these conditions, only $S_2O_5^{2-}$ was photolyzed. Figure 12 shows a representative oscilloscope trace and the transient spectrum measured 80 μsec and 1 sec after the flash. The long-lived absorption (curve b) closely resembles the spectrum of $S_2O_4^{2-}$ as measured in alkaline solution at 4° (curve c). (The small shift might be due to change in environment; a blue shift is usually induced by lowering temperature and increasing electrolyte concentration.) The formation of $S_2O_4^{2-}$ most likely proceeds by the following stages

$$^-O_3S\text{-}SO_2^- \xrightarrow{h\nu} SO_3^- + SO_2^- \qquad (15)$$

$$2SO_2^- \longrightarrow S_2O_4^{2-} \qquad (16)$$

It was not possible to observe SO_3^- because $S_2O_5^{2-}$ absorbs strongly below 300 nm (Figure 3), but a transient was detected at longer wavelengths that could be assigned to SO_2^-. Immediately after the flash, the spectrum revealed a band appearing as a shoulder on the long-wavelength side of the $S_2O_4^{2-}$ band, with λ_{max} ~365 nm (Figure 12, curve a). A band at 360 nm was measured[30] by diffuse reflectance spectrophotometry after X irradiation of solid dithionite, and was also assigned to SO_2^-.

The decay of SO_2^- proceeds in parallel with the buildup of $S_2O_4^{2-}$ (Figure 12). From the ratio between the parallel changes in absorbance (curves a and b), taking into account the stoichiometry (eq 16) and $\epsilon^{max}_{S_2O_4^{2-}} = 8300\ M^{-1}\ cm^{-1}$,[12] we could estimate $\epsilon^{max}_{SO_2^-} \lesssim 600\ M^{-1}\ cm^{-1}$. Only an upper limit is given because some SO_2^- might have reacted with SO_3^- to regenerate $S_2O_5^{2-}$.

The buildup of $S_2O_4^{2-}$ was found to be a second-order reaction. The kinetic expression applicable to this case is

$$\frac{1}{A_\infty - A_t} = \frac{2k_{16}t}{(\epsilon_{S_2O_4^{2-}}/2 + \epsilon_{SO_2^-})l} + \frac{1}{A_\infty - A_0} \qquad (17)$$

where A_0, A_t, and A_∞ are the absorbance values at times zero and *t* and at the end of the decay, at some specified wavelength; $\epsilon_{S_2O_4^{2-}}$ and $\epsilon_{SO_2^-}$ are the corresponding extinction coefficients; and *l* is the optical path (20 cm).

Applying eq 17 to our results, we obtained $2k_{16}/\epsilon^{330}_{S_2O_4^{2-}} = (2.2 \pm 0.2) \times 10^6$ (at 330 nm, $\epsilon_{SO_2^-}$ could be ignored), or $2k_{16} = (1.3 \pm 0.1) \times 10^{10}\ M^{-1}\ sec^{-1}$ (taking $\epsilon^{330}_{S_2O_4^{2-}} = 5700\ M^{-1}\ cm^{-1}$). These results refer to solutions of ionic strength $I \sim 0.1$ *M*. If reaction 16 really occurs as written with no protonated forms involved,[31] then simple correction for ionic strength effect leads to $2k_{16} = (1.0 \pm 0.1)\ 10^{10}\ M^{-1}\ sec^{-1}$ at $I = 0$.

The decay of SO_2^- was followed directly at 370 nm, where the absorption of $S_2O_4^{2-}$ could be ignored. However, the absorption of SO_2^- was too weak for determining its decay order: plots of both first- and second-order kinetics yielded straight lines. From the second-order plot, $2k_{16}/\epsilon_{370} \sim 2.5 \times 10^7$ was obtained; *i.e.*, $2k_{16} \lesssim 1.3 \times 10^{10}\ M^{-1}\ sec^{-1}$ (at $I \sim 0.1$ *M*). The upper limit is in agreement with the value obtained from the buildup of $S_2O_4^{2-}$, and this suggests that $\epsilon^{max}_{SO_2^-}$ is close to 600 M^{-1} cm^{-1}.

Reaction 16 could also be followed by studying the flash photolysis of $S_2O_4^{2-}$. In Figure 12 an oscilloscope trace is shown of the regeneration of $S_2O_4^{2-}$ decomposed

---

(29) M. C. R. Symons and S. B. Barnes, *J. Chem. Soc. A*, 2000 (1970).

(30) H. C. Clark, A. Horsfield, and M. C. R. Symons, *ibid.*, 7 (1961).

(31) L. Burlamacchi, G. Guerini, and E. Tiezzi, *Trans. Faraday Soc.*, 65, 496 (1969).

Table III. Spectral and Kinetic Data on the Oxyradicals of Sulfur

Radical	Spectral parameters		Reaction kinetics	$2k$, M^{-1} sec^{-1}	Ref
	λ_{max}, nm	ϵ_{max}, M^{-1} cm^{-1}			
SO_2^-	365	$\sim 6 \times 10^2$	$2SO_2^- \rightarrow S_2O_4^{2-}$	$1.0 \pm 0.1 \times 10^{10}$	*a*
SO_3^-	255	1.15×10^3	$2SO_3^- \rightarrow S_2O_6^{2-}$	$1.1 \pm 0.2 \times 10^9$	*a*
			$SO_3^- + O_2 \rightarrow SO_5^-$	$>10^9$	*a*
			SO_3^- + ethanol $\rightarrow$	$\leqslant 2 \times 10^3$	*a*
SO_4^-	450	1.1×10^3	$2SO_4^- \rightarrow S_2O_8^{2-}$	8.8×10^8	14b, 28a
			$SO_4^- + OH^- \rightarrow SO_4^{2-} + OH$	$6.5 \pm 1.0 \times 10^7$	*a*, 28a
			$SO_4^- + H_2O \rightarrow HSO_4^- + OH$	$<3 \times 10^3$ sec^{-1}	*a*
			$SO_4^- + SO_3^{2-} \rightarrow SO_4^{2-} + SO_3^-$	$\geqslant 5.3 \times 10^8$	*a*
			SO_4^- + methanol $\rightarrow$	$1.1 \pm 0.2 \times 10^7$	*c*
			SO_4^- + ethanol $\rightarrow$	$3.5 \pm 0.3 \times 10^7$	*c*
			SO_4^- + isopropyl alcohol $\rightarrow$	$4.6 \pm 0.2 \times 10^7$	*c*
			SO_4^- + *tert*-butyl alcohol $\rightarrow$	$9.1 \pm 1.0 \times 10^5$	*a*
SO_5^-	<250		$2SO_5^- \rightarrow$	$\sim 4 \times 10^8$	*a*
			SO_5^- + ethanol $\rightarrow$	$\leqslant 10^3$	*a*
$S_2O_2^-$	280	6.3×10^3 [b]	$2S_2O_2^- \rightarrow$	$2k/\epsilon = 5 \times 10^4$	5
$S_2O_3^-$	380	1.7×10^3	$2S_2O_3^- \rightarrow$	6.8×10^9	5

[a] This work. [b] Estimated from ref 5. [c] L. Dogliotti and E. Hayon, *J. Phys. Chem.*, **71**, 3802 (1967).

initially by the flash. The original absorption is not fully restored; this may be due to the thermal decomposition of $S_2O_4^{2-}$ which occurs during the measurement time (~5 sec). Here too the reaction appeared second order; by applying eq 17, we obtained $2k_{16}$ $(I = 0) = (5 \pm 2) \times 10^9$ M^{-1} sec^{-1} at 4°. The activation energy of diffusion-controlled reactions is ~3 kcal; therefore, assuming that reaction 16 is diffusion controlled, $2k_{16}$ $(I = 0) = 7 \pm 3 \times 10^9$ M^{-1} sec^{-1} at 15°. Thus, the two independent methods lead to nearly the same value for this rate constant, which is lower than 6.4×10^{10} M^{-1} cm^{-1}, the value inferred from the paper of Lynn, *et al.*[32]

(5) SO_4^- Radical. This has been subjected to extensive research (for a recent paper with references to some earlier works, see ref 33). Here we present some new data, pertaining to our discussion on the autoxidation mechanism of sulfite (see below). The SO_4^- radical was generated by the pulse radiolysis of $S_2O_8^{2-}$ in oxygen-free solutions[28a]

$$e_{aq}^- + S_2O_8^{2-} \longrightarrow SO_4^- + SO_4^{2-} \qquad (18)$$

The spectrum of SO_4^- (Figure 13) appears as an overlap of two bands. (We did not observe the double-band structure reported for the 450-nm band.[28a]) The reactions investigated and some previous data are recorded in Table III with their second-order rate constants. Because of the relatively slow thermal reaction between $S_2O_8^{2-}$ and sulfite, only a lower limit can be given for reaction 19, $k_{19} \geqslant 5.3 \times 10^8$ M^{-1} sec^{-1}.

$$SO_4^- + SO_3^{2-} \longrightarrow SO_4^{2-} + SO_3^- \qquad (19)$$

Some preliminary results on the analogous reaction with HSO_3^- indicate that $k(SO_4^- + HSO_3^-)$ is higher than k_{19} by at least a factor of 2.5.

The reaction of SO_4^- with *tert*-butyl alcohol is considerably slower than that with secondary or primary alcohols (Table III). Thus SO_4^- is more selective than OH radicals[22] in H-atom-abstraction reactions.

In alkaline solutions the decay of SO_4^- becomes faster and increases with increase in pH. In the presence of O_2 it leads to the formation[14b] of O_3^-. This was attributed to the conversion of SO_4^- into OH radicals in aqueous solutions. We have confirmed that the first-order rate constant for the decay of SO_4^- varies linearly[28a] with $[OH^-]$ (see Figure 13) and have obtained $k_{20} = 6.5 \pm 1.0 \times 10^7$ M^{-1} sec^{-1}, in good agreement with previous data.[28a,34]

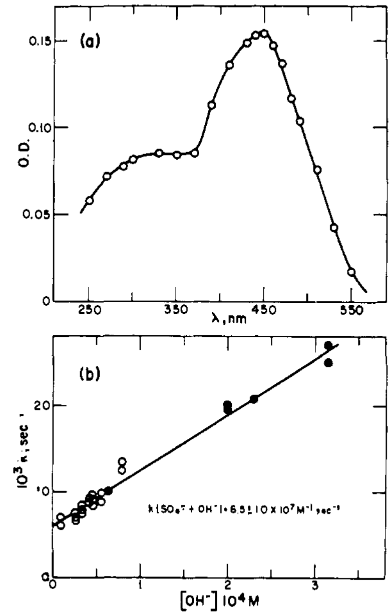

Figure 13. (a) Absorption spectrum of $SO_4^-\cdot$ radicals produced from the pulse rudiolysis of 2 m*M* $S_2O_8^{2-}$ ions, Ar (1 atm), pH 5.1. (b) Pseudo-first-order decay of $SO_4\cdot^-$ in oxygen-free alkaline solutions obtained from pulse radiolysis (●) and flash photolysis (○) data.

$$SO_4^- + OH^- \longrightarrow SO_4^{2-} + OH \qquad (20)$$

From the intercept of the line, an upper limit for the reaction

$$SO_4^- + H_2O \longrightarrow HSO_4^- + OH$$

could be determined, $k < 3 \times 10^3$ sec^{-1}. This result is in agreement with some previous estimates.[35] An upper limit only is given because the extrapolated rate

---

(32) S. Lynn, R. G. Rinker, and W. H. Corcoran, *J. Phys. Chem.*, **68**, 2363 (1964).

(33) I. Kraljic, *Int. J. Radiat. Phys. Chem.*, **2**, 59 (1970).

(34) L. Dogliotti and E. Hayon, *J. Phys. Chem.*, **71**, 3802 (1967).

(35) D. E. Pennington and A. Haim, *J. Amer. Chem. Soc.*, **90**, 3700 (1968).

Table IV. Spectral and Photochemical Data on the Oxyanions of Sulfur

Ion	Spectral parameters				Primary photochemical process	Ref
	λ_{max}, nm	ϵ_{max}, M^{-1} cm^{-1}	Transition	Ref		
SO_3^{2-}	$\leqslant 185$	$\sim 10^4$	Intramol	*a*	$SO_3^{2-} \rightarrow SO_3^- + e_{aq}^-$	*a*
HSO_3^-	190	4×10^3	CTTS	*a*	$HSO_3^- \rightarrow HSO_3 + e_{aq}^-$ (or $SO_3^- + H$)	*a*
SO_4^{2-}	175	3×10^2	CTTS	*b*	$SO_4^{2-} \rightarrow SO_4^- + e_{aq}^-$	*d*
HSO_5^-	<220			*a*	$HSO_5^- \rightarrow SO_4^- + OH(?)$	*a*
$S_2O_3^{2-}$	215	$\sim 2 \times 10^3$	CTTS	*c*	$S_2O_3^{2-} \rightarrow S_2O_3^- + e_{aq}^-$	5
					$\lambda < 215$	
					$\rightarrow S_2O_2^- + O^-$	5
	240	2×10^2	Intramol	*c*	$\rightarrow SO_3^- + S^-$	5, *e*
$S_2O_4^{2-}$	317	8.3×10^3		13, *a*	$S_2O_4^{2-} \rightarrow 2SO_2^-$	*a*
$S_2O_5^{2-}$	255	$\sim 4 \times 10^3$	Intramol	10, *a*	$S_2O_5^{2-} \rightarrow SO_3^- + SO_2^-$	*a*
$S_2O_6^{2-}$	<200			*a*	$S_2O_6^{2-} \rightarrow 2SO_3^-$	24, *a*
$S_2O_8^{2-}$	<200			*a*	$S_2O_8^{2-} \rightarrow 2SO_4^-$	14b, *a*

[a] This work. [b] J. T. Shapiro, Ph.D. Thesis, Bryn Mawr College, 1965. [c] R. Sperling and A. Treinin, *J. Phys. Chem.*, **68**, 897 (1964). [d] J. Barrett, M. J. Fox, and A. L. Mansell, *ibid.*, **69**, 2996 (1965); E. Hayon and J. J. McGarvey, *ibid.*, 71, 1472 (1967). [e] D. Behar and R. W. Fessenden, *ibid.*, **75**, 2572 (1971).

constant also includes some contributions from the bimolecular recombination of SO_4^- and reactions with impurities.

(C) The Autoxidation of Sulfite. Our results strongly support the view that SO_3^- and SO_5^- act as chain carriers in the oxidation of sulfite. According to Backstrom,[3c] SO_5^- acts by abstracting an H atom from HSO_3^-.

$$SO_5^- + HSO_3^- \longrightarrow HSO_5^- + SO_3^- \qquad (21)$$

Reaction 21 was proposed to explain the pH effect on the autoxidation of sulfite; it attains a maximum rate close to the pK of HSO_3^- (pH ~7).[4b,d] We have verified this pH effect by irradiating SO_3^{2-} and HSO_3^- at 2537 and 2288 Å, respectively. However, this explanation cannot be correct since in several cases (probably in the absence of inhibiting impurities) we observed an efficient chain reaction (high yield of e_{aq}^-) on flashing "air-containing" solutions of 5×10^{-3} M Na_2SO_3 at pH 12, where $[HSO_3^-] < 10^{-7}$ M. Under these conditions, the reaction $SO_5^- + SO_5^-$ (Table IV) should be faster than reaction 21 and therefore no chain reaction should occur. This mechanism can be modified by including reaction 22

$$SO_5^- + SO_3^{2-} \longrightarrow SO_5^{2-} + SO_3^- \qquad (22)$$

with $k_{22} < k_{21}$.

The formation of SO_4^{2-} was attributed[4b,d] to

$$HSO_5^- + SO_3^{2-} \longrightarrow HSO_4^- + SO_4^{2-} \qquad (23)$$

This reaction is probably slower than the chain-propagating reactions, which can account for the post effect observed in the photolysis of sulfite.[4c]

In the absence of inhibitors

$$SO_5^- + SO_5^- \longrightarrow \text{products} \qquad (24)$$

(or the analogous reaction with HSO_5) should be responsible for the chain termination; this reaction was studied experimentally (Table III). On the other hand, the propagation reaction which involves SO_5^- and SO_3^{2-} could not be followed because the regeneration of SO_5^- by the chain reaction is very fast. (In principle, this reaction could be studied in the absence of O_2 by producing SO_5^- from Caro's salt, but the latter rapidly reacts with sulfite.)

The main difficulty encountered by the Backstrom mechanism is concerned with the effect of alcohols: our results show that neither SO_3^- nor SO_5^- is efficiently scavenged by alcohols (Table III). We also carried out some experiments to measure the inhibition effect. The depletion of sulfite by flash-induced oxidation was measured in the absence and presence of alcohols. The following concentrations of alcohols were required to reduce the depletion to roughly about 30% of its value in alcohol-free solutions (using air-saturated 5×10^{-4} M Na_2SO_3 at pH 9.7): isopropyl alcohol, 4×10^{-5} M; ethanol, 1×10^{-4} M; methanol, 2×10^{-4} M; *tert*-butyl alcohol, 2×10^{-2} M. At these concentrations, the alcohols should react with some unknown chain carrier Y at a rate comparable to that of its termination reaction. We propose that Y is the SO_4^- radical and that the Backstrom mechanism should be modified by replacing reaction 22 by

$$SO_5^- + SO_3^{2-} \longrightarrow SO_4^- + SO_4^{2-} \qquad (25)$$

The SO_4^- radical produced then reacts according to reaction 19. The reasons for introducing the SO_4^- radical in the chain-reaction mechanism are as follows. (a) In their inhibition of the chain reaction, the alcohols appear to display selectivity which is roughly in agreement with the variation in rate constants k (alcohol + SO_4^-) (see Table III; the effect of *tert*-butyl alcohol is somewhat too low). (b) The drop of the oxidation rate at pH > p$K_{HSO_3^-}$ can be related to our observation that SO_4^- reacts with SO_3^{2-} more slowly than with HSO_3^-. (c) The sensitivity of autoxidation to inhibition is considerably higher in alkaline solutions. This fact, which became evident from our experiments by following the formation of e_{aq}^-, explains some conflicting data on the autoxidation in alkaline solutions.[4d] The reaction of SO_4^- with OH^- (reaction 20) replaces SO_4^- by OH, which can be more rapidly scavenged by impurities (*cf.*, *e.g.*, the rates of OH and SO_4^- with alcohols, Table III and ref 22). (d) We found striking evidence for the formation of OH (or O^- in alkaline solutions) by observing the intense spectrum of O_3^- (λ_{max} 430 nm, $\tau_{1/2} \sim 5$ msec) by flash photolysis of 10^{-2} M Na_2SO_3 saturated with O_2 at pH 12.9. Under these conditions, very little light is absorbed by OH^-. The pronounced slowing down of the autoxidation in highly alkaline solutions[4d] can be related to the slow reaction of O_3^- with SO_3^{2-} (a reaction which probably involves O^- and OH[36]).

---

(36) A. Treinin, *Isr. J. Chem.*, 8, 103 (1970).

In conclusion, we propose the following mechanism for the photoxidation of sulfite

Initiation

$$SO_3^{2-} \xrightarrow{h\nu} SO_3^- + e_{aq}^- \ (+ O_2 \longrightarrow O_2^-) \qquad (7)$$

$$SO_3^- + O_2 \longrightarrow SO_5^- \qquad (12)$$

Propagation

$$SO_5^- + SO_3^{2-} \longrightarrow SO_4^- + SO_4^{2-} \qquad (25)$$

$$SO_4^- + SO_3^{2-} \longrightarrow SO_4^{2-} + SO_3^- \qquad (19)$$

Termination

$$SO_5^- + SO_5^- \longrightarrow \qquad (24)$$

$$SO_4^- + SO_4^- \longrightarrow \qquad (26)$$

and other termination reaction (*e.g.*, $SO_5^- + O_2^- \rightarrow$). In the thermal autoxidation, the photochemical initiation is replaced by some other electron transfer, *e.g.*, to Cu^{2+}. This mechanism is applicable to systems where $[HSO_3^-]$ is small and the conversion of SO_4^- into OH can be ignored. Extension of the mechanism to include reactions of HSO_3^- and OH can account for the pH effect. In strongly alkaline solutions, SO_5^- and O^- are the main chain carriers of the autoxidation.

It is interesting to note that in alkaline solution the mechanism presented here bears some resemblance to the Haber mechanism[2] which involves the following chain-propagation reaction.

$$HSO_3 + O_2 + H_2O + SO_3^{2-} \longrightarrow 2SO_4^{2-} + OH + 2H^+ \qquad (27)$$

This reaction is the overall form (in acidic form) of reactions 12, 25, and 20.

Finally, it should be emphasized that we have no direct evidence for the role of SO_4^- in the autoxidation mechanism. Our efforts to detect its spectrum have failed. We believe that this is due to the low concentration of SO_4^- present in the system. If, for simplicity, we ignore the termination reactions and consider the steady concentrations of SO_5^- and SO_4^- in the system after the flash, then eq 25 and 19 lead to the relation $[SO_4^-] = (k_{23}/k_{19})[SO_5^-]$. There is no information on k_{25}, but because it involves oxygen transfer it is likely to be lower than k_{19}, *i.e.*, $[SO_4^-] < [SO_5^-]$. Both radicals have comparable extinction coefficient, and since the absorption of SO_5^- was rather weak (Figure 10), that of SO_4^- could have escaped detection. Here it is of interest to note that with their sensitive device to study the spectra of transient species produced in the steady photochemistry, Devonshire and Weiss[7] found some difference around 450 nm (λ_{max} of SO_4^-) between the spectra produced in oxygen and argon saturated solutions of Na_2SO_3.

Some Data on Oxyanions and Oxyradicals of Sulfur. Tables III and IV summarize some spectroscopic and kinetic data pertaining to the photochemistry of the oxyanions of sulfur. The following conclusions can be drawn from these tables. (a) The primary process occurring in ions with strong S–O bonds is electron ejection. (b) The single S–S and O–O bonds are readily ruptured. (c) The rate constants for the bimolecular recombination of the radicals SO_n^- decrease with increase in n.

Acknowledgment. We are indebted to Mrs. L. Dogliotti (Natick Laboratories) and Dr. I. Loeff (Hebrew University) for their assistance in carrying out some of the flash photolysis experiments.

ω-Type Calculations on π-Electron Systems with Inclusion of Overlap Charges. III. π-Bond Energies, Heats of Formation, and Resonance Energies of Conjugated Hydrocarbons

S. P. Gupta and B. Krishna

Contribution from the Department of Chemistry, University of Allahabad, Allahabad-2, India. *Received July 21, 1970*

Abstract: The ω technique with inclusion of overlap charges, as described in previous papers of this series, has been extended to evaluate the π-bond energies, heats of formation, and resonance energies of some conjugated hydrocarbons. The success of the method has been supported by comparing the results with experimental data and with results obtained by others using Pople's SCF–MO method.

Generally quantum chemists have used the ω technique for π-electron systems with neglect of overlap charges. However, as reported in our previous papers,[1,2] we have have performed ω-type calculations on π-electron systems with inclusion of overlap charges and consequently ionization potentials and electron affinities have been calculated for some conjugated hydrocarbons. The results have been found to be in good agreement with the observed values.

For the sake of simplicity in writing, the method has been abbreviated as the IOC-ω technique (inclusion of overlap charges in the ω technique) and, according to this method

$$H_{\mu\mu} = \alpha_0 + \omega\left[1 - \frac{1}{2}\sum_{\sigma}(p_{\mu\sigma}S_{\mu\sigma} + p_{\sigma\mu}S_{\sigma\mu})\right] \qquad (1)$$

$$H_{\mu\nu} = \frac{1}{2}KS_{\mu\nu}(H_{\mu\mu} + H_{\nu\nu}) \qquad (2)$$

Here α_0 is the core Coulomb integral which describes the energy of a π electron in a p_z atomic orbital in a

---

(1) B. Krishna and S. P. Gupta, *J. Amer. Chem. Soc.*, **92**, 7247 (1970).
(2) B. Krishna and S. P. Gupta, *J. Chem. Soc. A*, 123 (1971).